Hydrogen-Bonded Supramolecular Polymer Adhesives: Straightforward Synthesis and Strong Substrate Interaction

Senbin Chen, Zeke Li, Yanggui Wu, Nasir Mahmood, Frédéric Lortie, Julien Bernard, Wolfgang Binder, Jintao Zhu

Hydrogen-Bonded Supramolecular Polymer Adhesives: Straightforward Synthesis and Strong Substrate Interaction

Senbin Chen,*[a] Zeke Li,[a] Yanggui Wu,[a] Nasir Mahmood,[b] Frédéric Lortie,[c] Julien Bernard,[c] Wolfgang H. Binder,[d] Jintao Zhu*[a]

[a] Prof. Dr. S. Chen, Z. Li, Y. Wu, Prof. Dr. J. Zhu
Key Laboratory of Materials Chemistry for Energy Conversion and Storage, Ministry of Education (HUST), School of Chemistry and Chemical Engineering, Huazhong University of Science and Technology (HUST), Wuhan 430074, China
E-mail: senbin@hust.edu.cn (S. Chen), jtzhu@hust.edu.cn (J. Zhu)
[b] Dr. N. Mahmood
Institute of Chemistry, Chair of Macromolecular Chemistry, Faculty of Natural Sciences II, Martin-Luther University Halle-Wittenberg, Kurth-Mothes-Strasse 2, D-06120, Halle (Saale) D-06120, Germany
[c] Dr. F. Lortie, Dr. J. Bernard
Université de Lyon, CNRS, UMR 5223, Ingénierie des Matériaux Polymères, Université Lyon 1, INSA Lyon, UJM, F-69621 Villeurbanne cedex, France
[d] Prof. Dr. W. H. Binder
Institute of Chemistry, Martin-Luther University Halle-Wittenberg, von Danckelmann-Platz 4, D-06120, Halle (Saale), Germany.

Supporting information for this article is given via a link at the end of the document.

Abstract: High-performance adhesives are of great interest in view of industrial demand. We herein identify a straightforward synthetic strategy towards universal hydrogen-bonded (H-bonded) polymeric adhesives, using a side-chain barbiturate (Ba) and Hamilton wedge (HW) functionalized copolymer. Starting from a rubbery copolymer containing thiolactone derivatives, Ba and HW moieties are tethered as pendant groups via an efficient one-pot two-step amine-thiol-bromo conjugation. Hetero-complementary Ba/HW interactions thus yield H-bonded supramolecular polymeric networks. In addition to an enhanced polymeric network integrity induced by specific Ba/HW association, the presence of individual Ba or HW moieties enables strong binding to a range of substrates, outstanding compared to commercial glues and reported adhesives.

Introduction

Nature widely uses the power of supramolecular interactions as the driving force for various reversible adhesion phenomena, such as van der Waals forces in gecko footpads,[1] H-bonding, electrostatic interactions, and/or metal coordination in the secretions of tube worms or mussels.[2] Such supramolecular interactions are responsible for these macro/microscopic adhesions, to accomplish a variety of specific (bio)physical functions.[3-5]

Inspired by nature, scientists have developed sophisticated adaptive adhesion strategies via supramolecular interactions, placing, e.g., H-bonds,[6-12] macrocycle-based host-guest interactions,[3,13,14] metal-ligand coordination,[15] van der Waals forces, electrostatic interactions, hydrophobic interactions, and/or steric repulsion onto precisely designed (macro)molecules.[16] Acting as the ubiquitous interaction in complex living organisms, H-bonding forces have been exploited as one of the primary (macro)molecular interaction tools to fabricate a wide range of biomimetic materials. Recent studies have revealed that H-bonding forces play a crucial role in enhancing the mechanical properties and macroscopic adhesion behavior of supramolecular polymers.[6-10] As dynamic H-bonding interactions can be placed on diverse building blocks in apolar solvents and the bulk state, with their dynamic association/dissociation enabling energy dissipation in materials, they offer great potential to direct complexation processes, leading to adhesive materials with universal reversibility and self-healing capabilities.

Employing low molar mass bis-urea functionalized polyisobutylenes, Creton and Bouteiller[6,17] have developed supramolecular soft adhesives, showing interesting adhesive properties both on stainless steel surfaces but also on substrates with very low surface energies such as silicones. By utilizing 2-ureido-4[1 H]-pyrimidinone- (UPy-) moieties,[8,9] 2.7-diamidonaphthyridine (DAN)/ureido-7-deazaguanine (DeUG) quadruple H-bonding pair,[7] supramolecular materials with enhanced mechanical properties and a remarkable adhesive strength on diverse substrates have been reported.

Compared to the existing H-bonded supramolecular polymeric adhesives, a novel synthetic design and strategies thereto are continually sharpened. The association of hetero-complementary barbiturate (Ba) and Hamilton wedge (HW) into sextuple hetero-complementary H-bonding arrays has been studied by us[18-22] and others,[23-25] to reversibly bond together separated blocks, allowing the construction of supramolecular polymeric architectures, well-defined nanostructures, and self-healing materials. Although H-bonding interactions have been demonstrated to improve interfacial adhesion, the Ba/HW couple remains surprisingly unexplored in its bonding capability onto various substrates and in macroscopic adhesive applications.

In this study, we address the design and synthesis of side-chain Ba- and HW-functionalized P(*n*BuA-*co*-Ba-*co*-HW) random copolymer (**Figure 1**). We show that introducing Ba/HW moieties into polymeric adhesives leads to a strong, but reversible substrate binding system, considering its high binding with the association constant equal to 10^{4-5} M^{-1} in chloroform.[17] Typically, the random copolymerization of *n*BuA and TIaAm (thiolactone acrylamide) is conducted using reversible addition-fragmentation

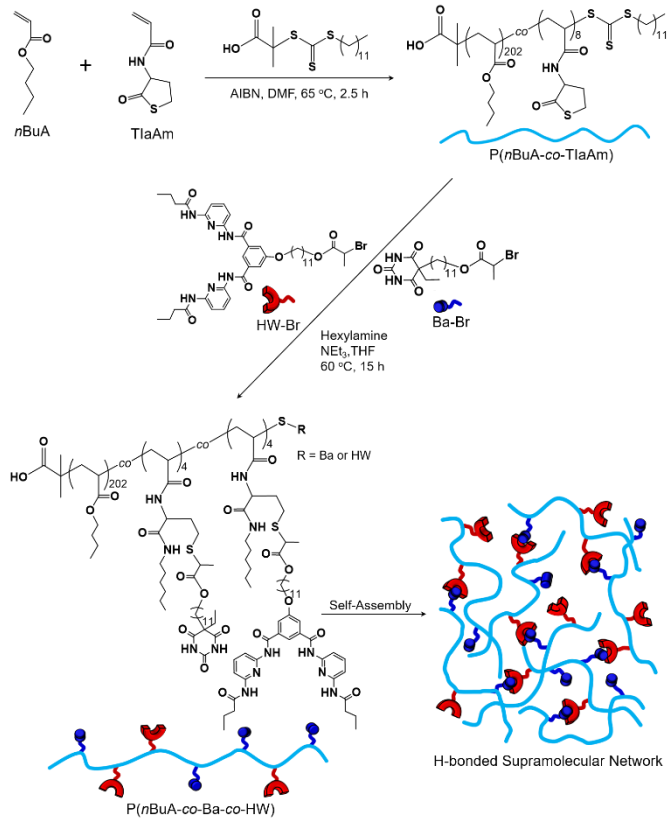

Figure 1: Synthetic route to the side-chain Ba- and HW-functionalized P(*n*BuA-*co*-Ba-*co*-HW) polymer and its self-assembly to afford the H-bonded supramolecular network.

chain-transfer (RAFT) technique, to afford P(*n*BuA-*co*-TIaAm) random copolymer. Subsequent ring-opening of thiolactone units generates reactive thiols which are then engaged in thiol-bromo click reactions to attach Ba and HW moieties.[26,27] This two-step approach provides the targeted P(*n*BuA-*co*-Ba-*co*-HW) copolymer with Ba and HW moieties randomly dispersed as side groups. This in turn enables the formation of H-bonding supramolecular networks, showing internally linked Ba-HW moieties. The strong yet dynamic Ba/HW interactions are anticipated to dissipate energy through the reversible association/dissociation of H-bonded complexes, contributing to the improved toughness of these supramolecular polymeric networks. Thus, the resulting P(*n*BuA-*co*-Ba-*co*-HW) can be exploited as supramolecular polymeric adhesives, where Ba/HW interactions serve as both promoters (e.g., cohesive domains) maintaining the H-bonded polymeric network integrity between two substrates, in addition to the linkers bound onto the substrates via H-bonding interactions (e.g., adhesive domains).

Results and Discussion

Polymeric materials with integrated structure functionalities are demanded to match the designed practical applications; however, there is always a trade-off between the complex material performance and the synthetic simplification. Herein, we present a straightforward and effective synthetic strategy to transform a viscous liquid-like polymer, P(*n*BuA-*co*-TIaAm), into a viscoelastic supramolecular polymeric material, P(*n*BuA-*co*-Ba-*co*-HW), featuring high processability and strong adhesion to various surfaces.

Aiming at fabricating the side-chain Ba- and HW-functionalized P(*n*BuA-*co*-Ba-*co*-HW) polymer (**Figure 1**), we have first prepared a random copolymer P(*n*BuA-*co*-TIaAm) ($M_{n\ NMR}$ = 27.3 kg/mol, $M_{n\ SEC}$ = 30.6 kg/mol, $Đ$ = 1.25), using 2-(dodecylthiocarbonothioylthio)-2-methylpropionic acid (DDMAT) as chain transfer agent and RAFT polymerization.[23,25-27] The theoretical number-average molar mass ($M_{n\ th}$ = 25.5 kg/mol), evaluated from the monomers' conversion, is consistent with the experimental ones ($M_{n\ NMR}$ and $M_{n\ SEC}$) and proves the controlled character of such RAFT copolymerization. The introduction of TIaAm monomer together with *n*-butyl acrylate (*n*BuA) allows to precisely tune the glass-transition as well as the hydrophilic/hydrophobic balance of the resulting H-bonding polymer. The thiolactone moieties as the latent thiol functionality are randomly introduced into the polymer chain via the RAFT copolymerization with *n*BuA, allowing post-polymerization modification via thiol-based click reactions.[28-31] Compared to the TIaAm feeding ratio in the comonomer mixtures (f_{TIaAm} = 0.051), the slightly lower molar fraction of TIaAm monomer in the final copolymers (F_{TIaAm} = 0.038) suggests that TIaAm monomer is slightly less reactive than the *n*BuA monomer. Thiolactone chemistry is known as a versatile platform for the generation of multifunctional polymers. Indeed, by combining ring-opening of thiolactone unit via a primary amine and the subsequent conversion of the *in situ* generated thiols through thiol-ene/yne,[28,30,32-34] thiol-bromo,[35] and thiol-epoxy[36] reactions, scientists have synthesized a wide range of polymers via such efficient one-pot double modification strategy recently.

In this study, P(*n*BuA-*co*-TIaAm) is treated with hexylamine in the presence of Ba-Br and HW-Br, thus allowing the one-pot two-step amine-thiol-bromo conjugation reaction. The thiolactone side groups of P(*n*BuA-*co*-TIaAm) form thiols via the nucleophilic ring-opening reaction with hexylamine, directly randomly reacting *in-situ* with bromoester-functionalized Ba and HW moieties (Ba-Br or HW-Br) in a one-pot fashion. The resulting P(*n*BuA-*co*-Ba-*co*-HW) is purified by precipitation into methanol/water (1/1, v/v). The successful chemical modification of P(*n*BuA-*co*-TIaAm) into P(*n*BuA-*co*-Ba-*co*-HW) is firstly supported by size exclusion chromatography (SEC, **Figure S1**, $M_{n\ NMR}$ = 33.5 kg/mol, $M_{n\ SEC}$ = 36.7 kg/mol, $Đ$ = 1.29), as the shift towards higher molar mass is attributed with the tethering of Ba-Br and HW-Br compounds.

^{1}H NMR analysis is further performed to prove the attachment of Ba and HW moieties via the amine-thiol-bromo conjugation reactions (**Figure 2**). Compared to the spectrum of the starting P(*n*BuA-*co*-TIaAm) copolymer (**Figure 2**a), a slight shift of the C*H* proton (initially belonging to the thiolactone group) from 4.63 to 4.54 ppm, S-CH_2- protons from 3.26 to 3.15 ppm, along with the emergence of Ba imide protons (10.47 ppm in **Figure 2**b), HW imide protons (9.45 and 9.04 ppm in **Figure 2**b), as well as the phenyl and pyridyl protons (8.02 and 7.67 ppm in **Figure 2**b) indicates the successful linking of Ba and HW moieties onto the polymer chain. Notably, the comparable integrations between Ba (10.47 ppm) and HW (8.02 and 7.67 ppm ppm) imide protons demonstrate that equal amounts of Ba and HW moieties are attached (about 4 of each H-bonding motif per chain) to afford P(*n*BuA-*co*-Ba-*co*-HW), thus indicating a similar reactivity of Ba-Br and HW-Br toward nucleophilic substitution (**Figure 2**). The

addition of hexylamine also triggers the aminolysis of trithiocarbonate end group, as supported by the complete

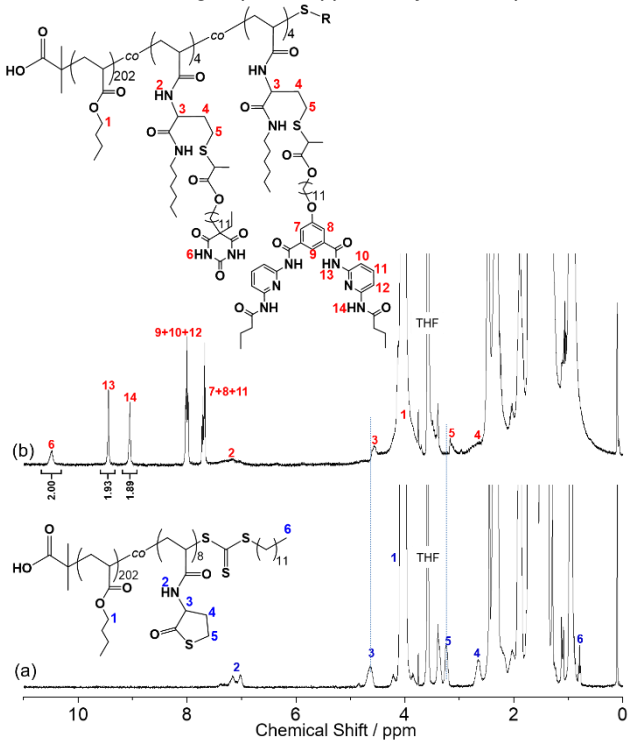

Figure 2: ^{1}H NMR spectra of (a) P(*n*BuA-*co*-TIaAm), and (b) P(*n*BuA-*co*-Ba-*co*-HW), recorded in THF-d_8 at 27 °C.

disappearance of the characteristic ω-methyl end group (0.81 ppm). The *in-situ* generated reactive thiols are anticipated to randomly react with Ba-Br or HW-Br, thus leading to either Ba or HW moieties attached as the ω-end groups of P(*n*BuA-*co*-Ba-*co*-HW).

Fourier-transform infrared (FT-IR) spectral analysis is then performed to study the H-bonding behavior of P(*n*BuA-*co*-Ba-*co*-HW) copolymer (**Figure 3**). Spectra of the N-H stretching region of P(*n*BuA-*co*-Ba-*co*-HW) are given as a function of temperature. The H-bonded N-H stretching band between N-H and C=O due to the Ba/HW interaction is observed at 3324 cm^{-1} at 30 °C. The N-H band shifts gradually from 3324 to 3350 cm^{-1} upon heating from 30 to 150 °C (**Figure 3**a), revealing a significant weakening of H-bonds with increasing temperatures. Importantly, the N-H stretching band progressively shifts back to its initial position by cooling from 150 down to 30 °C (**Figure 3**b), indicative of the successful reformation of the H-bonding complex.

Figure S2 shows comparative zero shear viscosities of P(*n*BuA-*co*-TIaAm) and P(*n*BuA-*co*-Ba-*co*-HW) between 0 and 100 °C. In both cases, the values decrease with increasing temperatures.

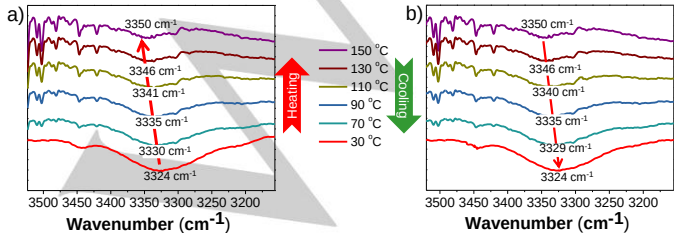

Figure 3: Temperature-dependence of FT-IR spectra (a: heating, b: cooling) for N-H stretching vibrations of P(*n*BuA-*co*-Ba-*co*-HW) copolymer.

Surprisingly, only a slight decrease of viscosity is observed from P(*n*BuA-*co*-Ba-*co*-HW) upon heating, revealing a thermally stable H-bonded supramolecular polymer network due to the strong Ba/HW association. The representative temperature-dependent shear moduli G' and G" are shown in **Figure S3**. To study in details the impact of H-bonds, master curves of P(*n*BuA-*co*-TIaAm) and P(*n*BuA-*co*-Ba-*co*-HW) are plotted. A standard time-temperature superposition has been performed to build a frequency master curve at a reference temperature of 20 °C. In the standard analysis of time-temperature superposition, and to rescale all the obtained linear frequency-dependent shear results, T-dependent shifting factors (a_T) are shown in **Figure S4**. The linear oscillatory frequency-sweep spectrum of the starting P(*n*BuA-*co*-TIaAm) exhibits a typical viscous liquid-like behavior, showing predominantly greater loss moduli (G") than storage moduli (G') over the entire frequency range (**Figure 4**a). A distinct behavior is observed from P(*n*BuA-*co*-Ba-*co*-HW), showing that the storage moduli, G', are constantly greater than the loss moduli, G". Moreover, both G' and G" straightens out and scales with $\omega^{0.5}$ against the rescaled angular frequency (ωa_T) over nearly 4 orders of magnitude (**Figure 4**b). This viscoelastic behavior strongly suggests a gel state. The exceedingly broad spectrum of overlapping G' and G" without a terminal relaxation time reveals a stable gelatinous network structure (over the explored temperature range), which is undoubtedly ascribed to the robust H-bonding interactions of the Ba/HW pairs.

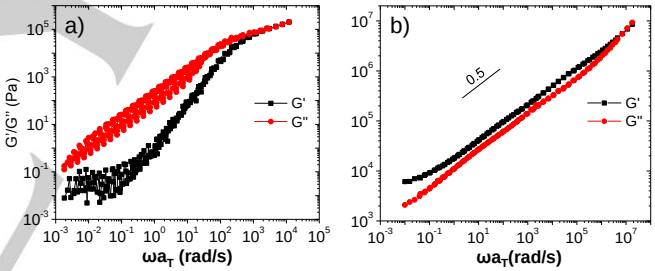

Figure 4: Time-temperature superposition master curves of shear moduli G' and G" for: (a) P(*n*BuA-*co*-TIaAm), (b) P(*n*BuA-*co*-Ba-*co*-HW) against shifted angular frequency ωaT.

The bulk structural morphologies of the P(*n*BuA-*co*-TIaAm) and P(*n*BuA-*co*-Ba-*co*-HW) copolymers are subsequently investigated via small angle x-ray scattering (SAXS). P(*n*BuA-*co*-TIaAm) does not show any scattering peak, while P(*n*BuA-*co*-Ba-*co*-HW) exhibits a sharp peak at 0.403 nm^{-1} along with a shoulder, suggesting the presence of disordered micelles with a diameter of 15.7 nm (**Figure S5**). The formation of these aggregates stems from the establishment of multiple of H-bonded polymeric crosslinking nodes. DSC analysis is carried out to further investigate the phase segregation of P(*n*BuA-*co*-TIaAm) and P(*n*BuA-*co*-Ba-*co*-HW) copolymers. As shown in **Figure S6**, the DSC trace for P(*n*BuA-*co*-TIaAm) displays a clear glass transition temperature (T_g) at -37 °C. Interestingly, P(*n*BuA-*co*-Ba-*co*-HW) copolymer displays two distinct thermal transitions. In addition to the transition at -37 °C relative to the T_g of P(*n*BuA-*co*-TIaAm) copolymer, another weak transition is observed at 49 °C which is believed to arise from the interchain association driven by Ba/HW H-bonding interactions.[37]

The adhesive properties of P(*n*BuA-*co*-Ba-*co*-HW) are first investigated on glass surfaces as is customarily done for viscoelastic adhesives. P(*n*BuA-*co*-Ba-*co*-HW) solution using

THF as solvent (20 mg/mL) is deposited on a glass slide, to obtain approx. 1 mm-thick films after 24 h of air drying at 30 °C, followed by 48 h of vacuum drying at 60 °C to completely extract the solvent. Then another glass plate is hot-pressed on that adhesive film at 60 °C with a contact force of 70 N to produce a constant layer with a thickness of *ca.* 0.1 mm. Subsequent cooling to room temperature for 24 h enables the uniform contact and firm bonding to substrates. Remarkably, a weight of as high as 10.8 kg can be steadily hung up through the two adhered glass slides with the glued volume of 25 × 27 × 0.1 mm (**Figure 5**a). In contrast, P(*n*BuA-*co*-TIaAm) which is not equipped with H-bonding moieties to bind the substrate interfaces and which displays a viscous liquid-like behavior, systematically failed to glue the tested substrates.

To quantitatively understand the adhesive performance of P(*n*BuA-*co*-Ba-*co*-HW), stress-strain curves obtained from the normalizing force and displacement of the contact area are shown in **Figure 5**b, with de-bonding velocity ranging from 10 to 1000 μm·s^{-1}. It is clear that P(*n*BuA-*co*-Ba-*co*-HW) is highly viscoelastic, as the peak of stress increases strongly with increasing probe velocity, a behavior expected for the viscoelastic materials.[5] Subsequent progressive decrease of stress after the climax is an indication of a load bearing elongational viscosity, which can be ascribed to the H-bonded Ba/HW crosslinking along with a strong binding and adhesive to the surface of substrate. At last, the rupture occurs at the polymer-glass interface suggesting an adhesive failure mode.

Subsequently, the temperature-dependent adhesive performance is investigated at a de-bonding velocity of 100 μm·s^{-1}. As shown in **Figure 5**c, adhesive properties of P(*n*BuA-*co*-Ba-*co*-HW) decrease as temperature increases from 25 to 60, finally to 90 °C. Such result is qualitatively expected, since the level of viscoelastic dissipation during strain decreases with increasing temperature. As anticipated, similar conclusions are drawn with different de-bonding velocities.

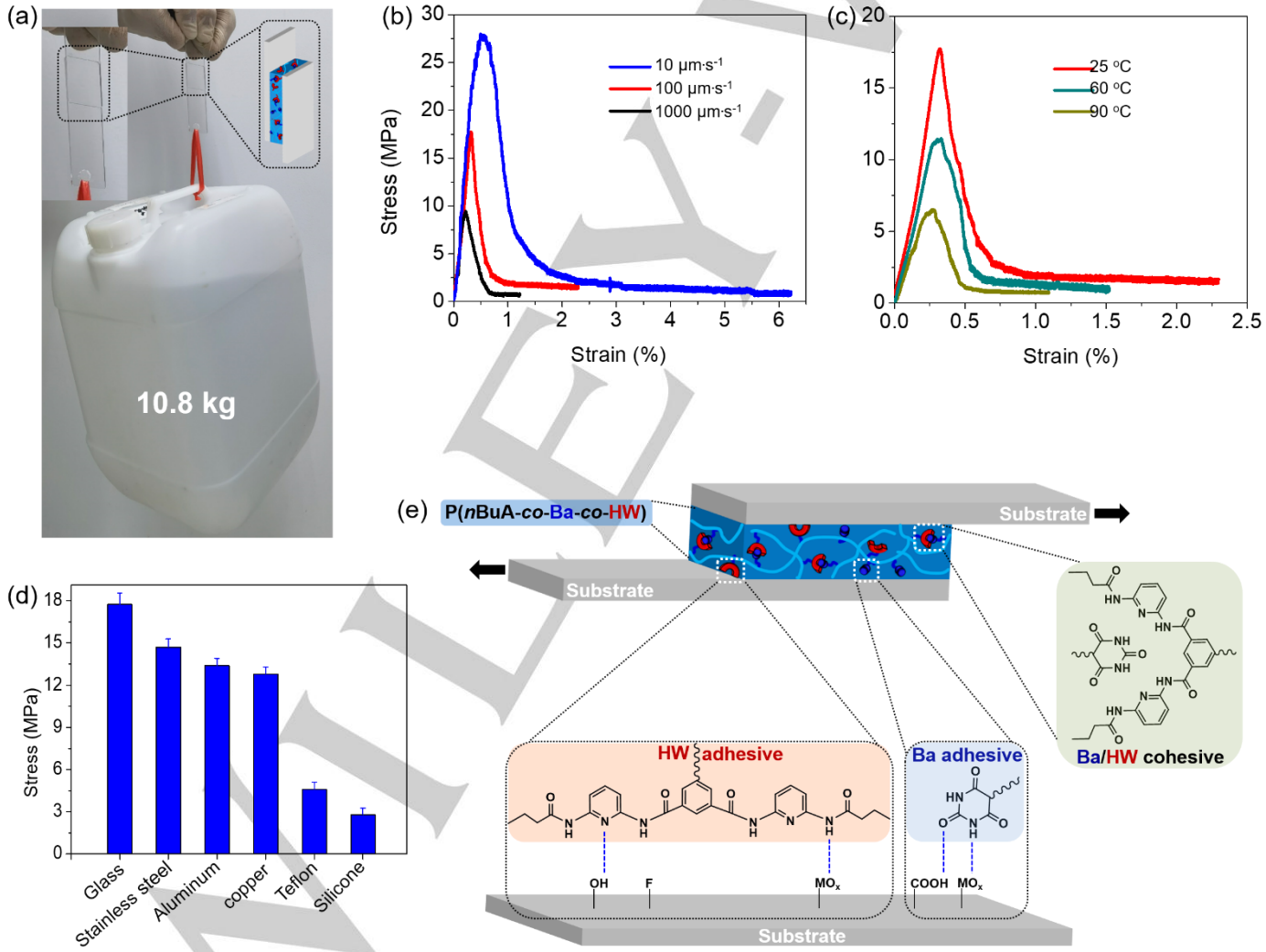

Figure 5: Photograph demonstrating that the glass slides adhered by P(*n*BuA-*co*-Ba-*co*-HW) can hold a weight of 10.8 kg with a lap joint area of 25 × 27 × 0.1 mm (a), stress-strain curves for P(*n*BuA-*co*-Ba-*co*-HW) as adhesives at a de-bonding speeds of 10, 100, 1000 μm·s^{-1} at 25 °C (b), at 25, 60, 90 °C with de-bonding speeds of 100 μm·s^{-1} (c), shear stress for different substrates including glass, stainless steel, aluminium, copper, Teflon and silicone rubber at a de-bonding speeds of 100 μm·s^{-1} at 25 °C (d), and schematic of the dynamic interfacial gluing between P(*n*BuA-*co*-Ba-*co*-HW) and substrate through diverse H-bonding (e).

It is important to test whether the adhesive capability of P(*n*BuA-*co*-Ba-*co*-HW) works well on different substrates. Therefore, the glass slides are subsequently replaced by stainless steel, aluminum, copper, hydrophobic Teflon, and silicone rubber, respectively, followed by the same protocol with a de-bonding velocity of 100 μm·s^{-1}. Stress-stain curves demonstrate that a shear strength of higher than 12 MPa is recorded for all glass and metallic substrates (**Figure 5**d), superior to commercial 3M glues and most adhesive materials that have been reported.[8] This high shear strength may be ascribed to i) the good internal cohesion of the sandwiched P(*n*BuA-*co*-Ba-*co*-HW) polymer layer due to the formation of H-bonding complexes between Ba and HW motifs in the bulk and ii) the strong adhesion of free Ba and HW motifs at the polymer/substrate interface, which can form H-bonds with either the hydroxyl groups of glass surfaces, or oxygen of metallic oxide layers (MO_x, **Figure 5**e) on the top of the substrates.[10]

Although the adhesion experiments on glass and metal surfaces are informative on the differences in large strain performance brought by the H-bonding forces, they are not the sole consequence of interfacial interactions, as van der Waals forces at the polymer/glass and polymer/metal oxide interfaces are also sufficiently strong to deform the adhesively elastic layer remarkably.[38] The situation is rather different if the adhesive layers are de-bonded from a hydrophobic, low surface energy surfaces, such as Teflon or silicone rubber with which hydrogen-bonds are not expected to occur. The shear stresses of P(*n*BuA-*co*-Ba-*co*-HW) detaching from Teflon and silicone surface are determined to be 4.6 and 2.8 MPa respectively (**Figure 5**d). Although slightly lower than that measured on glass and metal surfaces, the obtained shear strengths are still outstanding compared to the commercial glues and the adhesive materials described in previous reports.[3,4] Other adhesion mechanisms are certainly involved to explain such acceptable bonding performances. It is noteworthy that the strength of adhesion on Teflon is greater than on silicone rubber. Such result can be explained by a model of adhesion where the viscoelastic adhesive undergoes slippage along a rigid solid interface, where Teflon surface is more rigid than flexible PDMS.[39,40]

These remarkable results emphasize the significance of the heterocomplementary Ba/HW interactions in P(*n*BuA-*co*-Ba-*co*-HW) not only serving as promoters (e.g., cohesive domains, **Figure 5**e) to maintain the H-bonded polymeric network integrity between two substrates, but also favorably effecting the rheological properties of viscoelastic layer by making it more dissipative. The Ba and HW moieties are able to link onto the substrates via diverse H-bonding interactions (e.g., adhesive domains, **Figure 5**e), forming strong interactions especially onto glass and metallic substrates.[41] It is proven that, used as an additive, such Ba and HW moieties as strongly H-bonding interacting groups could significantly enhance the adherence even onto difficult-to-bind surfaces, highlighting the versatility of P(*n*BuA-*co*-Ba-*co*-HW) as universal adhesives.

Conclusion

In summary, we have demonstrated a rational design of a promising platform for creating strong polymeric adhesive materials. We firstly challenge the synthesis of side-chain Ba and HW moieties functionalized P(*n*BuA-*co*-Ba-*co*-HW) via efficient one-pot two-step amine-thiol-bromo conjugation, then elucidating the dynamic behavior and relaxation lifetime of Ba/HW interactions driven supramolecular assemblies in the melt state, revealing P(*n*BuA-*co*-Ba-*co*-HW) to behave as a critical gel, finally ascertaining H-bonded supramolecular polymeric adhesives of various substrates (e.g., glass, stainless steel, aluminum, copper, Teflon and silicone rubber). Effective energy dissipation from the bulk H-bonded polymeric networks, and superior adhesion strength through diverse H-bonding interactions are the key factors that result in the tough bonding. This strategy provides a new and effective route to fabricate H-bonded adhesive materials and engineer strong substrate interaction. We envision that not only the design strategy of post-modified multi-functionalized polymers can be adopted in the advances of supramolecular polymeric architectures, but macroscopic interfacial adhesion via such dynamic Ba/HW interactions to be applied in practical application fields, such as wearable and stretchable electronics, hybrid biomedical devices, and tissue/bone adhesives.

Acknowledgements

This work is funded by the National Natural Science Foundation of China (52173253 and 21801085). W. H. B. thanks the DFG Research Training Group RTG/GRK 2670, TP B2 Dr 43649874 for financial support. We thank the HUST Analytical and Testing Centre for allowing us to use the facilities.

Keywords: Hydrogen bonds • Amine-thiol-bromo conjugation • Self-assembly • Supramolecular polymeric adhesives

(1) Autumn, K.; Liang, Y. A.; Hsieh, S. T.; Zesch, W.; Chan, W. P.; Kenny, T. W.; Fearing, R.; Full, R. J. *Nature* **2000**, *405*, 681-685.
(2) Flammang, P.; Santos, R. *Interface Focus* **2015**, *5*, 20140086.
(3) Ji, X.; Ahmed, M.; Long, L.; Khashab, N. M.; Huang, F.; Sessler, J. L. *Chem. Soc. Rev.* **2019**, *48*, 2682-2697.
(4) Shi, C.-Y.; Zhang, Q.; Tian, H.; Qu, D.-H. *SmartMat.* **2020**, *1*, e1012.
(5) Heinzmann, C.; Weder, C.; de Espinosa, L. M., *Chem. Soc. Rev.* **2016,** *45*, 342-358.
(6) Courtois, J.; Baroudi, I.; Nouvel, N.; Degrandi, E.; Pensec, S.; Ducouret, G.; Chanéac, C.; Bouteiller, L.; Creton, C. *Adv. Funct. Mater.* **2010**, *20*, 1803-1811.
(7) Anderson, C. A.; Jones, A. R.; Briggs, E. M.; Novitsky, E. J.; Kuykendall, D. W.; Sottos, N. R.; Zimmerman, S. C. *J. Am. Chem. Soc.* **2013**, *135*, 7288-7295.
(8) Faghihnejad, A.; Feldman, K. E.; Yu, J.; Tirrell, M. V.; Israelachvili, J. N.; Hawker, C. J.; Kramer, E. J.; Zeng, H. *Adv. Func. Mater.* **2014**, *24*, 2322-2333.
(9) Ji, X.; Shi, B.; Wang, H.; Xia, D.; Jie, K.; Wu, Z. L.; Huang, F. *Adv. Mater.* **2015,** *27*, 8062-8066.
(10) Liu, M.; Wang, Z.; Liu, P.; Wang, Z.; Yao, H.; Yao, X. *Sci. Adv.* **2019**, *5*, eaaw5643.
(11) Peng, Q.; Chen, J.; Zeng, Z.; Wang, T.; Xiang, L.; Peng, X.; Liu, J.; Zeng, H. *Small* **2020**, *16*, 2004132.
(12) Wu, S.; Cai, C.; Li, F.; Tan, Z.; Dong, S. *CCS Chem.* **2021**, *3*, 1690-1700.
(13) Wang, H.; Zhu, C. N.; Zeng, H.; Ji, X.; Xie, T.; Yan, X.; Wu, Z. L.; Huang, F. *Adv. Mater.* **2019,** *31*, 1807328.

(14) Zhang, M.; Xu, D.; Yan, X.; Chen, J.; Dong, S.; Zheng, B.; Huang, F. *Angew. Chem. Int. Ed.* **2012,** *51*, 7011-7015.
(15) Zhang, Q.; Shi, C.-Y.; Qu, D.-H.; Long, Y.-T.; Feringa, B. L.; Tian, H. *Sci. Adv.* **2018**, *4*, eaat8192.
(16) De Greef, T. F. A.; Smulders, M. M. J.; Wolffs, M.; Schenning, A. P. H. J.; Sijbesma, R. P.; Meijer, E. W. *Chem. Rev.* **2009**, *109*, 5687-5754.
(17) Callies, X.; Véchambre, C.; Fonteneau, C.; Herbst, F.; Chenal, J. M.; Pensec, S.; Chazeau, L.; Binder, W. H.; Bouteiller, L.; Creton, C. *Soft Matter* **2017**, *13*, 7979-7990.
(18) Chen, S.; Rocher, M.; Ladaviere, C.; Gerard, J.-F.; Lortie, F.; Bernard, J., *Polym. Chem.* **2012,** *3*, 3157-3165.
(19) Chen, S.; Binder, W. H. *Acc. Chem. Res.* **2016**, *49*, 1409-1420.
(20) Chen, S.; Yan, T.; Fischer, M.; Mordvinkin, A.; Saalwächter, K.; Thurn-Albrecht, T.; Binder, W. H. *Angew. Chem. Int. Ed.* **2017**, *56*, 13016-13020.
(21) Chen, S.; Geng, Z.; Zheng, X.; Xu, J.; Binder, W. H.; Zhu, J. *Polym. Chem.* **2020**, *11*, 4022-4028.
(22) Chen, S.; Wu, Y.; Wang, H.; Zhu, B.; Xiong, B.; Binder, W. H.; Zhu, J. *Polym. Chem.* **2021**, *12*, 4111-4119.
(23) Fischer, T. S.; Schulze-Sünninghausen, D.; Luy, B.; Altintas, O.; Barner-Kowollik, C. *Angew. Chem. Int. Ed.* **2016**, *55*, 11276-11280.
(24) Elacqua, E.; Croom, A.; Manning, K. B.; Pomarico, S. K.; Lye, D.; Young, L.; Weck, M. *Angew. Chem. Int. Ed.* **2016**, *55*, 15873-15878.
(25) Douarre, M.; Martí-Centelles, V.; Rossy, C.; Tron, A.; Pianet, I.; McClenaghan, N. D. *Supramol. Chem.* **2020**, *32*, 546-556.
(26) Chen, S.; Ströhl, D.; Binder, W. H. *ACS Macro Lett.* **2015**, *4*, 48-52.
(27) Chen, S.; Lechner, B.-D.; Meister, A.; Binder, W. H. *Nano Lett.* **2016**, *16*, 1491-1496.
(28) Espeel, P.; Goethals, F.; Du Prez, F. E. *J. Am. Chem. Soc.* **2011**, *133*, 1678-1681.
(29) Reinicke, S.; Espeel, P.; Stamenović, M. M.; Du Prez, F. E. *ACS Macro Lett.* **2013**, *2*, 539-543.
(30) Zhang, H.; Wu, W.; Zhao, X.; Zhao, Y. *Macromolecules* **2017**, *50*, 3411-3423.
(31) Frank, D.; Espeel, P.; Claessens, S.; Mes, E.; Du Prez, F. E. *Tetrahedron* **2016**, *72*, 6616-6625.
(32) Zhang, Z.; Tan, Z.-B.; Hong, C.-Y.; Wu, D.-C.; You, Y.-Z. *Polym. Chem.* **2016**, *7*, 1468-1474.
(33) Yan, J.; Wang, R.; Pan, D.; Yang, R.; Xu, Y.; Wang, L.; Yang, M. *Polym. Chem.* **2016**, *7*, 6241-6249.
(34) Rudolph, T.; Espeel, P.; Du Prez, F. E.; Schacher, F. H. *Polym. Chem.* **2015**, *6*, 4240-4251.
(35) Chen, Y.; Espeel, P.; Reinicke, S.; Du Prez, F. E.; Stenzel, M. H. *Macromol. Rapid Commun.* **2014**, *35*, 1128-1134.
(36) Mommer, S.; Truong, K.-N.; Keul, H.; Moller, M. *Polym. Chem.* **2016**, *7*, 2291-2298.
(37) Chen, S.; Deng, Y.; Chang, X.; Barqawi, H.; Schulz, M.; Binder, W. H. *Polym. Chem.* **2014**, *5*, 2891-2900.
(38) Crosby, A. J.; Shull, K. R.; Lakrout, H.; Creton, C. *J. Appl. Phys.* **2000**, *88*, 2956-2966.
(39) Newby, B.-m. Z.; Chaudhury, M. K.; Brown, H. R., *Science* **1995,** *269*, 1407-1409.
(40) Zhang, Y.; Anderson, C. A.; Zimmerman, S. C. *Org Lett* **2013,** *15*, 3506-3509.
(41) Amouroux, N.; Petit, J.; Léger, L. *Langmuir* **2001**, *17*, 6510-6517.

Entry for the Table of Contents

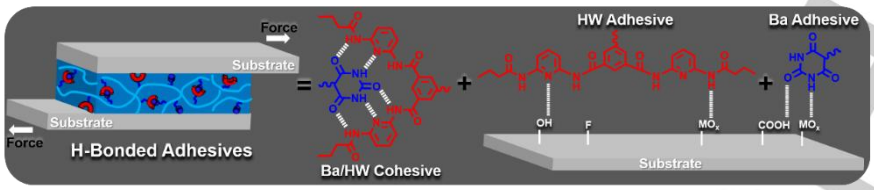

A straightforward synthetic strategy towards strong supramolecular adhesives is reported, based on a side-chain barbiturate (Ba) and Hamilton wedge (HW) functionalized polymer. Specific Ba/HW interactions serve as cohesive domains to maintain polymeric network integrity, while molecular configuration of individual Ba or HW moieties linked onto substrates via diverse H-bonding interactions, form adhesive domains and endow strong adherence.